Supplementary Materials: Semiconducting p-Type Copper Iron Oxide Thin Films Deposited by Hybrid Reactive-HiPIMS + ECWR and Reactive-HiPIMS Magnetron Plasma System

Zdenek Hubička [1,*], Martin Zlámal [2], Jiri Olejníček [1], Drahoslav Tvarog [1], Martin Čada [1] and Josef Krýsa [2,*]

[1] Institute of Physics, Division of Optics, Academy of Sciences of the Czech Republic, Na Slovance 2, 182 21 Prague, Czech Republic; olejnj@fzu.cz (J.O.); twarogd@fzu.cz (D.T.); cadam@fzu.cz (M.C.)

[2] Department of Inorganic Technology, University of Chemistry and Technology Prague, Technicka 5, 166 28 Prague, Czech Republic; zlamalm@vscht.cz

* Correspondence: hubicka@fzu.cz (Z.H.); krysaj@vscht.cz (J.K.)

1. Plasma Diagnostics by Radio Frequency (RF) Planar Probe

A plasma diagnostic at conditions of reactive r-HiPIMS and r-HiPIMS + ECWR depositions were done by a so-called radio frequency (RF) planar probe, which is described in detail in reference [34]. This method has origin in Sobolewski method presented in [35–37]. The base of this diagnostics is in the measurement of RF current I_{RFp} and RF voltage U_{RFp} on a planar probe connected to separate an RF generator through the blocking capacitor. The frequency of this generator should be lower than ion plasma frequency [34]. In our experiments the frequency of this generator was set up on f = 350 kHz. The basic experimental arrangement of this diagnostics method used in this paper can be seen in Figure S1. The planar RF probe is placed at the position of the substrate in the distance 150 mm from the surfaces of both targets. The RF generator is connected through a blocking capacitor C to a planar probe through a sensor containing a current transformer Tr_1 and capacitive voltage probe P_{vc} (Figure S1). Signals from current transformer Tr_1 and voltage probe P_{vc} are fed to digital storage oscilloscope and $I_{RFp}(t)$ with $U_{RFp}(t)$ waveforms can be obtained and transferred from the scope to PC for further software processing. The example of obtained I_{RFp} and U_{RFp} during the active discharge r-HiPIMS pulse on copper magnetron cathode can be seen in Figure S2. Ion flux on the probe I_0 can be obtained from I_{RFp} at time t_0 when U_{RFp} has minimum value. At this time, all electrons are repelled from the probe and simultaneously $\frac{dU_{RFp}}{dt}(t_0) = 0$. It means that both capacitive current i_c and electron current i_e at the probe for this moment are i_c = 0, I_e = 0 respectively. The capacitive current through the probe can be expressed as

$$i_c = C_p(U_{RFp})\frac{dU_{RFp}}{dt}(t) \qquad (1)$$

where $C_p(U_{RFp})$ includes dynamical capacitance of the sheath on the probe and parasitic capacitance of the probe relative to ground.

Since $\frac{dU_{RFp}}{dt}(t_0) = 0$, we can state that $i_c(t_0) = 0$.

For this reason, at time t_0, it is valid that: $I_{RFp}(t_0) = I_0$ [35]. Ion flux I_0 is the ion saturation current on negative biased planar probe. Ion flux density $i_{ionflux}$ can be calculated if we know the surface S_p of the probe according to the following formula:

$$i_{ionflux} = \frac{I_0}{S_p} \qquad (2)$$

S_p = 0.5 cm^2 in our experimental configuration. In order to avoid edge effect on the planar probe, we have used the guard electrode around the circular active planar probe (Figure S2), which is on the same potential as the active probe, but the I_{RFp} was measured only through the active probe and was not measured through the guard electrode. This method was already presented in reference [38,39]. This method improves the accuracy of the calculation of $i_{ionflux}$. As we have many periods of U_{RFp} during r-HiPIMS pulse, we can calculate $i_{ionflux}$ with good time resolution $\tau = \frac{1}{f} \approx 2.9\ \mu s$ during the r-HiPIMS pulse since we can get the value of $i_{ionflux}$ only once per one period of U_{RFp} signal on the probe.

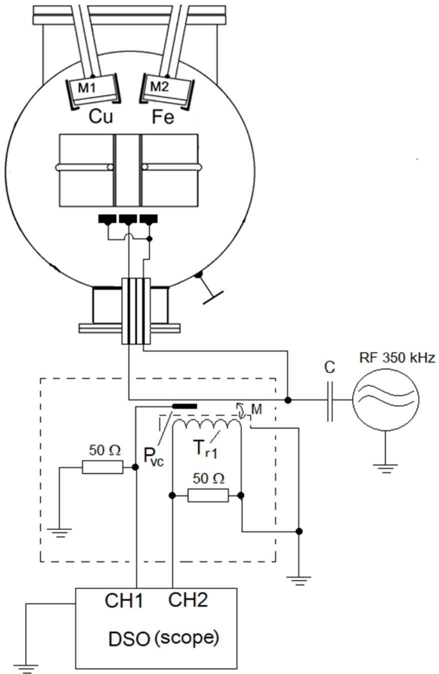

Figure S1. Experimental configuration of guarded planar radio frequency (RF) probe for measurement of current and voltage waveforms and plasma diagnostics.

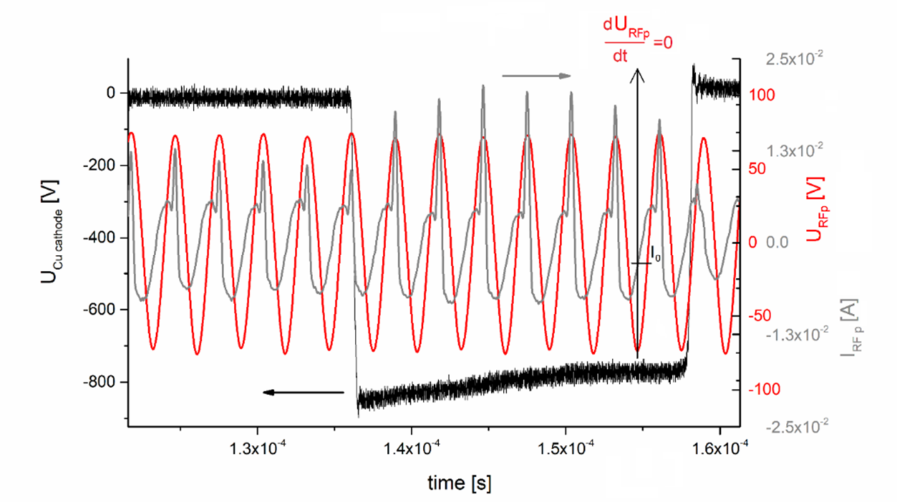

Figure S2. The example of time evolution of RF current $I_{RFprobe}$ RF voltage $U_{RFprobe}$ measured on the RF planar probe. Time evolution of cathode voltage on Cu cathode is shown as well in case of reactive r-HiPIMS + ECWR deposition copper iron oxide with P_{ECWR} = 180 W.

This method can be used also when the surface of the probe is coated with insulating or semiconductor layer. This insulating layer exhibits a further capacitor in serious with the probe circuit which introduces only a small impedance for the measured RF current I_{RFp}. This is valid if the deposited layer on the probe is thin enough [35].

The ion flux density $i_{ionflux}$ can be used for plasma ion concentration n_i calculation according to the following approximate formula [40]:

$$i_{ionflux} = e \times n_i \times \sqrt{\frac{k_B T_e}{M_i}} \tag{3}$$

where e is the charge of the electron, n_i is the ion concentration, k_B is the Boltzman constant, T_e is the electron temperature and M_i is the mass of heavy ions.

In order to be able to calculate n_i from (3), it is necessary to know T_e. The method of how to get from $I_{RFp}(t)$ and $U_{RFp}(t)$ on the planar probe parts of Langmiur probe characteristics in the region of ion saturation current and in the region around the floating potential is presented in reference [34]. The fundament of this method is the subtracting of capacitive current presented in Equation (1) from the total probe current.

$$I_p(t)=I_{RFp}(t)-C_p(U_{RFp})\frac{dU_{RFp}}{dt}(t) \tag{4}$$

If we take a single period of $U_{RFp}(t)$ and $I_{RFp}(t)$ from the particular minimum of U_{RFp} to the next minimum, we can reconstruct two functions of I_{RFp} (U_{RFp}), as can be seen in Figure S3, where the first function can be created for $\frac{dU_{RFp}}{dt} > 0$ as

$$I_{RFp} = I_{SA}(U_{RF}) = I_p(U_{RFp}) + C_p(U_{RFp})\frac{dU_{RFpA}}{dt}(U_{RFp}) \tag{5}$$

and the second function can be created for $\frac{dU_{RFp}}{dt} < 0$ as

$$I_{RFp} = I_{SB}(U_{RF}) = I_p(U_{RFp}) + C_p(U_{RFp})\frac{dU_{RFpB}}{dt}(U_{RFp}) \tag{6}$$

From Equations (5) and (6), we can calculate for each particular U_{RFp} the desired $I_p(U_{RFp})$ and $C_p(U_{RFp})$ as $\frac{dU_{RFpB}}{dt}$, $\frac{dU_{RFpA}}{dt}$, I_{SA}, I_{SB} are known quantities which can be directly calculated from measurement. In Figure S3, we can see the final calculated $I_p(U_{RFp})$ for particular U_{RFp} period, and this is the desired part of Langmuir probe characteristics for plasma parameters calculation.

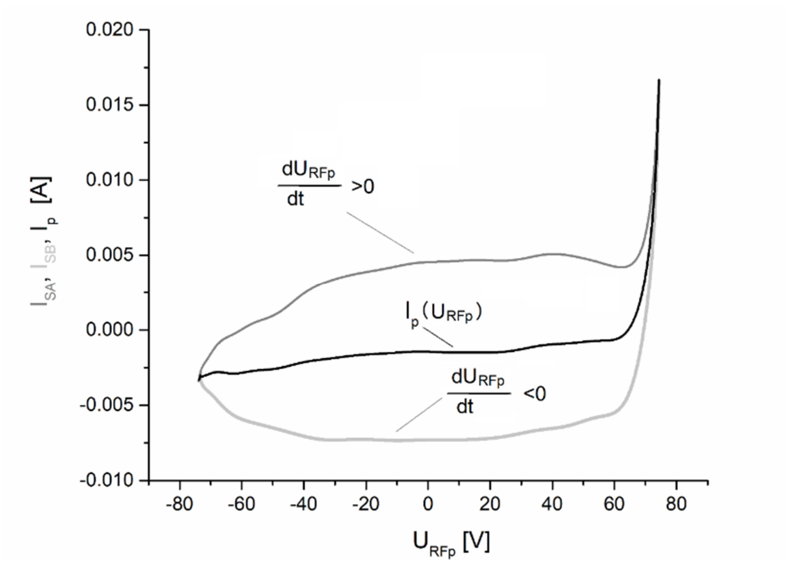

Figure S3. Example of reconstructed current voltage characteristics for the single U_{RFp} voltage sweep in the middle of copper discharge pulse in case of reactive r-HiPIMS + ECWR deposition copper iron oxide with P_{ECWR} = 180 W.

One simple possibility for how to get the electron temperature T_e from $I_p(U_{RFp})$ for the ideal planar probe is to calculate the second derivative of probe current to get the electron energy probability function and from the slope of the function $\ln \frac{d^2 I_p}{dU_{RFp}^2}(U_{RFp})$.

We can get the electron temperature T_e [40]. This approach is valid only in case of existence of Maxwellian electron distribution function in the plasma. This is not often true. In the case of non-Maxwellian electron distribution function, we get the so-called tail electron temperature that describes only the electrons with energies around floating potential U_{fl} [39]. In Figure S4, we can see an example of tail electron temperature T_e calculation in the middle of active discharge pulse on the copper magnetron cathode in hybrid r-HiPIMS + ECWR plasma excitation.

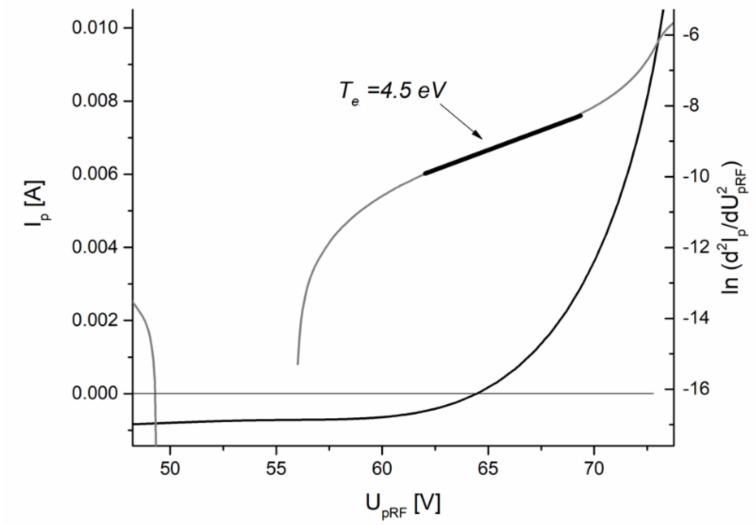

Figure S4. Example of reconstructed current voltage characteristics for the single U_{RFp} voltage sweep in the middle of copper pulse in case of reactive r-HiPIMS + ECWR deposition copper iron oxide with P_{ECWR} = 180 W, logarithm of second derivative is shown with fitted electron temperature T_e from the tail of electron distribution function.

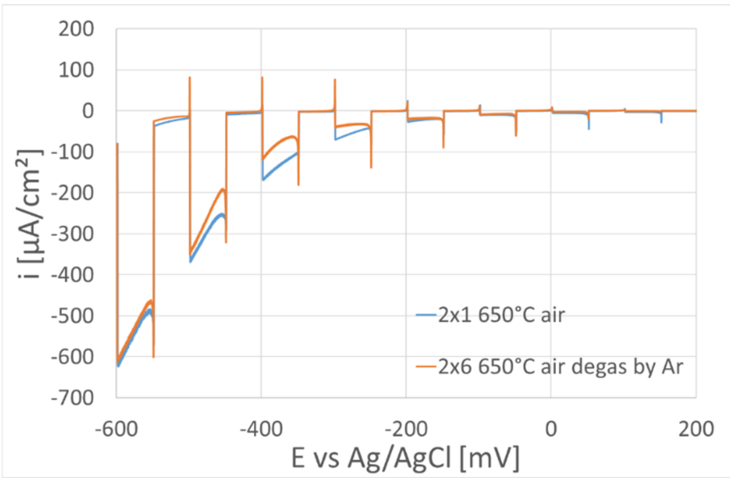

Figure S5. Linear voltammetry of the sample 2x annealed in air on 650 °C in electrolyte without degassing by argon and in electrolyte degassed by flow of argon for 5 h before PEC measurement.

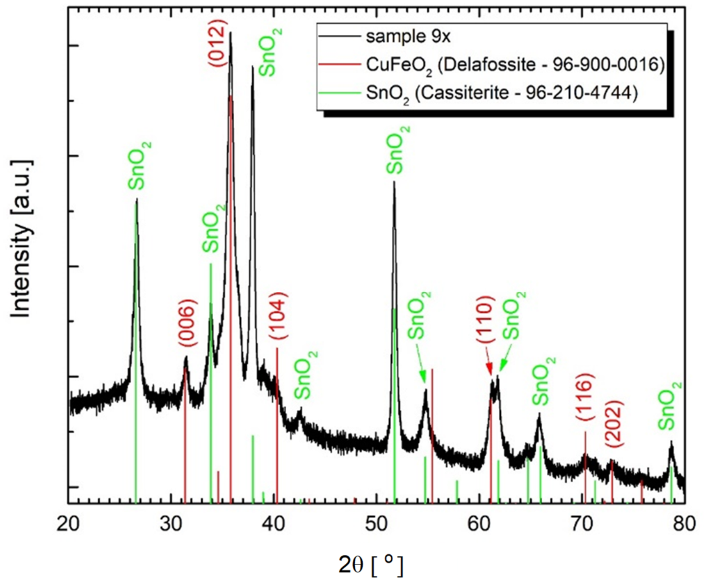

Figure S6. X-ray diffraction (XRD) of sample 9x with significant delafossite structure after annealing of the sample after deposition at 650°C in vacuum.

References

34. Sezemský, P.; Straňák, V.; Kratochvíl, J.; Čada, M.; Hippler, R.; Hrabovský, M.; Hubicka, Z. Modified high frequency probe approach for diagnostics of highly reactive plasma. *Plasma Sources Sci. Technol.* **2019**, *28*, 115009, doi:10.1088/1361-6595/ab506c.
35. Sobolewski, M.A. Measuring the ion current in electrical discharges using radio-frequency current and voltage measurements. *Appl. Phys. Lett.* **1998**, *72*, 1146–1148, doi:10.1063/1.121032.
36. Sobolewski, M.A. Measuring the ion current in high-density plasmas using radio-frequency current and voltage measurements. *J. Appl. Phys.* **2001**, 90, 2660, doi:10.1063/1.1390491.
37. Sobolewski, M.A.; Lahr, D.L. Origin of electrical signals for plasma etching end point detection: Comparison of end point signals and electron density. *Vac. Sci. Technol. A* **2012**, *30*, 051303, doi:10.1116/1.4737615.
38. Murali, D.S.; Kumar, S.; Choudhary, R.J.; Wadikar, A.D.; Jain, M.K.; Subrahmanyam, A. Synthesis of Cu_2O from CuO thin films: Optical and electrical properties. *AIP Adv.* **2015**, *5*, 047143, doi:10.1063/1.4919323.
39. Booth, J. P., Braithwaite, N. St. J., Goodyear, A., & Barroy, P. Measurements of characteristic transients of planar electrostatic probes in cold plasmas. Rev. Sci. Instrum. **2000**, *71*, 2722, doi: 10.1063/1.1150681.
40. Lienermann, M.A.; Lichtenberg, A.J. *Principles of Plasma Discharges and Materials Processing*, 2nd ed.; John Wiley and Sons., New York, NY, USA, 2003, doi:10.1002/0471724254.

© 2020 by the authors. Licensee MDPI, Basel, Switzerland. This article is an open access article distributed under the terms and conditions of the Creative Commons Attribution (CC BY) license (http://creativecommons.org/licenses/by/4.0/).